Parametric Optimization of Experimental Conditions for Dye-Sensitized Solar Cells based on Far-red Sensitive Squaraine Dye

Takuya Morimoto, Naotaka Fujikawa, Yuhei Ogomi, Shyam S. Pandey, Shuzi Hayase

Graduate School of Life Science and Systems Engineering, Kyushu Institute of Technology, 2-4 Hibikino, Wakamatsu, Kitakyushu 808-0196, Japan

E-mail: morimoto-takuya@edu.life.kyutech.ac.jp; shyam@life.kyutech.ac.jp

Abstract. A far-red sensitive unsymmetrical squaraine dye SQ-41 has been synthesized and subjected to the fabrication of dye-sensitized solar cells by varying the various parameters in order attain optimum photoconversion efficiency (η). It has been demonstrated that an optimum ratio of dye to coadsorber, thickness of mesoporous TiO_2 layer, redox electrolyte and surface treatment are necessary to enhance overall external η. In the case of surface treatment, it has been shown to exhibit pronounced device performance when both of the FTO as well mesoporous TiO_2 surfaces were treated with aqueous $TiCl_4$. In spite of very high molar extinction coefficient of dye SQ-41, 10-12 μm thickness of mesoporous TiO_2 was found to be necessary to attain the maximum η.

1. Introduction

Dye sensitized solar cells (DSSCs) consisted of dye-adsorbed mesoporous TiO_2 as photoanode, Pt coated transparent conductive oxide (TCO) glass as cathode and a suitable electrolyte have been emerged as low cost next generation solar cells with minimal adverse impact on environment during its fabrication [1]. Research and development on various aspects of DSSCs in the last about 20 years led to the achievement of photoconversion efficiency (η) over 11 % even with sensitizers having photon harvesting mainly in the visible region of the solar spectrum [2-3]. Solar spectrum is consisted of photons from varying wavelengths encompassing from ultraviolet to infra-red (IR). Nearly quantitative photon harvesting in the visible wavelength reason has already been achieved by potential organic sensitizers indicating the need for development of suitable sensitizing dyes having efficient photon harvesting in the higher wavelength region [4-5]. To enhance the external power conversion efficiency even higher, it is highly desired to develop novel and efficient sensitizing dyes that can harvest photons from far-red to NIR wavelength region. Utilization of such dyes in combination with already developed as well as commercially available potential visible light absorbing sensitizers in hybrid or tandem DSSC architecture is expected to enhance the overall efficiency of the DSSCs.

In this context, squaraine dyes serve as one of the model representatives fulfilling this demand owing to very sharp and narrow light absorption that can be tuned from visible to IR wavelength region by judicious molecular design [6]. In past two decades after inception of DSSCs, a lot of works have been conducted for optimizing various DSSC fabrication parameters using visible light absorbing dyes in

Content from this work may be used under the terms of the Creative Commons Attribution 3.0 licence. Any further distribution of this work must maintain attribution to the author(s) and the title of the work, journal citation and DOI.
Published under licence by IOP Publishing Ltd

order to enhance the η [7]. NIR dyes are typically different as compared to their visible light absorbing dye counterparts due to narrow full width at half maximum and very high molar extinction coefficients. Therefore, such optimization parameters can be partially applied for NIR dyes due to their intense light absorption and enhanced aggregation behaviour owing to their relatively planer molecular structure and extended π-conjugation. This article deals with the influence of various DSSC fabrication parameters such as thickness of mesoporous TiO_2 layer, surface treatment, concentration of the dye-aggregating agent chenodeoxycholic acid (CDCA) and nature of redox electrolyte upon the photovoltaic behaviour using a model far-red squaraine dye SQ-41. Structures of dye SQ-41 and CDCA have been shown in the inset of Fig. 1.

2. Materials and Methods

Far-red sensitive unsymmetrical squaraine dye (SQ-41) has been synthesized and its structure has been characterized as per our earlier publication [8]. Electronic absorption spectra of the dye in ethanol solution as well as thin film of dye absorbed on mesoporous TiO_2 has been measured using UV-visible spectrophotometer (JASCO, V670). DSSC was fabricated using Ti-nanoxide D/SP and HT/SP pastes (Solaronix) on fluorine doped tin-oxide (FTO) glass by doctor blading followed by backing at 450°C for 30 min. This coating and backing process was repeated multiple times to prepare TiO_2 coated FTO substrates of variable thicknesses (2 - 20 μm). In order to optimize the surface properties of FTO and TiO_2 layers, $TiCl_4$ surface treatment was also conducted. This surface treatment was performed by dipping the substrates in 40 mM solution $TiCl_4$ in water at 70°C for 30 minutes followed by the backing at 500°C for 30 min. This makes a very thin and compact TiO_2 layer on the substrates. The TiO_2 coated FTO substrate thus obtained was subjected to dye adsorption at room temperature for 4 hours. Dye bath solution for dye adsorption was prepared by making 0.2 mM dye solution in ethanol using 10 mM of CDCA as dye aggregation preventing agent. This optimum ratio of dye to CDCA was selected based on our previous publication using this dye [9]. A thin catalytic layer of Pt was coated on FTO glass to use as counter electrode. Three different kind of iodine based redox electrolytes (**A, B** and **C**) have been used to see the implication of the constituents and their relative concentration as per the recipe in the reported literatures [10-12].

Electrolyte **A** was consisted of I_2 (0.05 M), LiI (0.5 M), 1,2-dimethyl-3-propylimidazolium iodide (0.6M) and t-butylpyridine (TBP, 0.5 M) in acetonitrile [10]. Electrolyte **B** was consisted of I_2 (0.05 M), LiI (0.5 M), 1,2-ethyl-3-methylimidazolium dicyanamide (0.6M) and TBP (0.6 M) in acetonitrile [11]. Electrolyte **C** was consisted of I_2 (0.05 M), LiI (0.5 M), 1,3-dimethylimidazolium iodide (0.5M), Guanadinium thiocyanate (0.1 M) and TBP (0.5 M) in a mixture of acetonitrile and valeronitrile (85:15) [12]. A 25 μm thick Himilan film (Mitsu-Dupont) was used as hot melt spacer. Device area of (0.2025 cm^2) was precisely controlled using a black metal mask on the DSSC during the photovoltaic measurements every time. Photovoltaic performance of DSSC thus fabricated was measured with a solar simulator (CEP-2000, Bunko Keiki, Japan) equipped with Xenon lamp for the light exposure. The spectrum of the solar simulator and its power were adjusted to be at global air mass 1.5 condition (100 mW/cm^2) using a spectroradiometer (LS-100, Eiko Seiki, Japan). Photocurrent action spectra of the solar cells were also measured with a constant photon flux of 1 x 10^{16} photons/cm^2 using an action spectrum measurement system connected to the solar simulator.

3. Results and Discussion

3.1. Photophysical Characterization

Figure 1 shows the electronic absorption and fluorescence emission spectra of sensitizing dye SQ-41 in ethanol solution along with the thin film adsorbed on mesoporous TiO_2. Electronic absorption spectrum shows a sharp absorption maximum (λ_{max}) at 634 nm with very high molar extinction coefficient of 1.98 x 10^5 $dm^3.mol^{-1}.cm^{-1}$ which is associated with the π-π* electronic transition with a small vibronic shoulder around 590 nm. At the same time, emission spectrum shows slightly red-shifted emission maximum at 642 nm having very small Stoke shift of 8 nm. This spectral behaviour is a typical characteristic of squaraine dyes and very small Stoke shift indicates the conformational rigidity of this

molecule in the excited state. On the other hand, electronic absorption spectrum of this dye in solid state shows a little bathochromically shifted λ_{max} of 647 nm along with spectral broadening. This is attributed to the interaction of dye with TiO_2 in the condensed state.

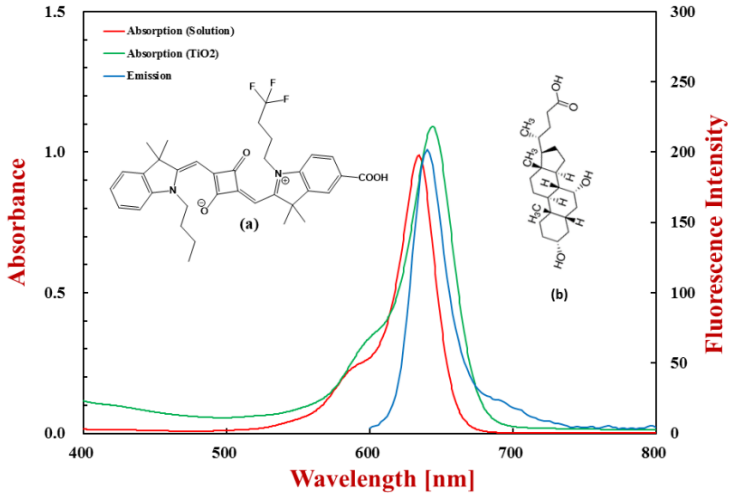

Figure 1. Electronic absorption spectra of SQ-41 in ethanol solution (5 μM), thin film on mesoporous TiO_2 and fluorescence emission spectrum in ethanol solution (1 μM). Inset shows the molecular structure of sensitizer SQ-41(a) and coadsorber CDCA (b).

3.2. Influence of $TiCl_4$ Surface Treatment

Photoanode in DSSC is consisted of FTO/TiO_2/dye interfaces and is the most important component of DSSCs which must be optimised for optimum device performance. Actually mesoporous TiO_2 is composed of interconnected nanoparticles which provides very high internal surface area promoting the high dye loading. At the same time, these interconnected TiO_2 nanoparticles offer not only limitation to facile electron transport but also charge recombination with electrolyte ions also. Since it is mesoporous in nature and electrolyte ions are also in contact with FTO surface, it offers the possibility of charge recombination between FTO and electrolyte ions also. To circumvent these problems application of a very thin layer of compact TiO_2 on FTO as well as TiO_2 has been found to be beneficial and used by many DSSC researchers. Surface treatment using aqueous $TiCl_4$ followed by backing is one of the most commonly used methods to prepare very thin compact layer of TiO_2. Apart from charge recombination blocking layer, this compact TiO_2 layer has been reported to play various roles like to increase the TiO_2 surface area [13], to enhance electron transport [14], to promote light scattering [15] and dye anchoring [16] finally leading to enhanced overall device performance. In this work, attempts have been made to investigate the role of this compact layer on overall device performance and demonstrate that which one plays the predominant role. In order to predict this effect more explicitly, other factors such as thickness of mesoporous TiO_2 layer (12-14 μm), dye (SQ-41), dye/CDCA ratio (1/50) and electrolyte (Electrolyte B) were kept the same.

Figure 2 shows the current-voltage (I-V) characteristics of DSSCs based SQ-41 having different surface treatment conditions under simulated solar irradiation along with the photovoltaic parameters in terms of short circuit current density (J_{sc}), open circuit voltage (V_{oc}), fill factor (FF) and η are summarized in the table 1. It can be clearly seen from this figure and table 1 that surface treatment of FTO has only little effect on η while surface treatment on mesoporous TiO_2 layer leads to drastic improvement of J_{sc} from 4.15 mA/cm^2 to 7.04 mA/cm^2 as compared to that obtained for without any surface treatment. Best DSSC performance with external power conversion efficiency 3.54 % was obtained when both of the FTO and TiO_2 surfaces were subjected to $TiCl_4$ surface treatment. In order to explain this profound enhancement of Jsc upon surface treatment, photocurrent action spectra also known as plot of incident photon to current conversion efficiency (IPCE) as a function of wavelength

of monochromatic light irradiation was also measured and has been shown in the Fig. 2. Action spectra shown in Fig. 2 clearly reveal the far-red photon harvesting by sensitizers and maxima of the observed IPCE is in accordance with the Jsc measured in the I-V characteristics.

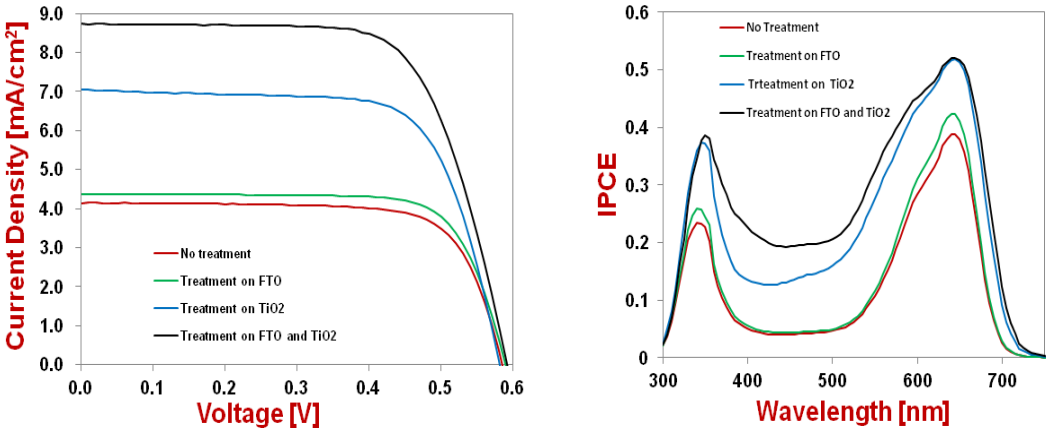

Figure 2. Photovoltaic characteristics of DSSCs under simulated solar irradiation (left) and photocurrent action spectra (right) after monochromatic incident light for DSSCs with different types of $TiCl_4$ surface treatments.

Table 1. Photovoltaic parameters for DSSC based on SQ-41 having $TiCl_4$ surface treatments conducted on different surfaces of photoanode.

Treatment Conditions	Efficiency (%)	FF	V_{oc} (V)	J_{sc} (mA/cm^2)
No surface Treatment	1.79	0.74	0.58	4.15
Treatment on FTO glass only	1.93	0.75	0.59	4.37
Treatment on TiO_2 layer only	2.88	0.70	0.58	7.04
Treatment on FTO glass and TiO_2 layer both	3.54	0.69	0.59	8.74

3.3. Thickness of Mesoporous TiO_2 Layer

Sensitizing dyes play most important role of photon harvesting in DSSCs. In order to have sufficient photon harvesting, mesoporous TiO_2 has been most extensively used for adsorption of dyes owing to its wide band gap and very high surface area. To achieve the best performance of DSSC an optimum thickness of the TiO_2 layer is highly desired. Lower thickness leads to non-optimal dye loading while too high thickness hampers the diffusion of redox species through the nanopores promoting the chances of charge carrier recombination. This optimal thickness depends on the nature of dye as well as particle size and preparation conditions of the mesoporous TiO_2. Using Ruthenium complex based dyes (N-719) Kang et al have demonstrated the need of 15 μm thick TiO_2 layer for best efficiency [17]. On the other hand, Yamaguchi et al used 34 μm thick mesoporous TiO_2 for the optimum efficiency of DSSC using Black dye [18]. Thus an optimization of TiO_2 layer thickness especially for this class of dyes is highly desired owing to their very high molar absorption coefficient where relatively thinner films are capable of absorbing sufficient photons. Keeping this in mind, DSSCs were fabricated by varying the thickness of mesoporous TiO_2 layer keeping other variables like dye, dye concentration, surface treatment, electrolyte (Electrolyte B), CDCA concentration etc. constant. Fig. 3 exhibits a typical I-V characteristic of the DSSC having the TiO_2 layer thickness of 10 μm giving a power conversion efficiency of 3.39 % under simulated solar irradiation. Photovoltaic characteristics of the DSSCs for other thicknesses of

TiO_2 were also measured and photovoltaic parameters in terms of J_{sc}, V_{oc}, FF and η are summarized in the table 2. A perusal of the inset of Fig. 2 indicating thickness dependence of η reveals that increase in the thickness leads to fast increase in the η up to about 10-14 μm and starts a sharp decline after 14 μm. This indicates at least 10 μm of mesoporous TiO_2 thickness is needed to achieve optimum efficiency in spite of such a high molar extinction coefficient of this dye.

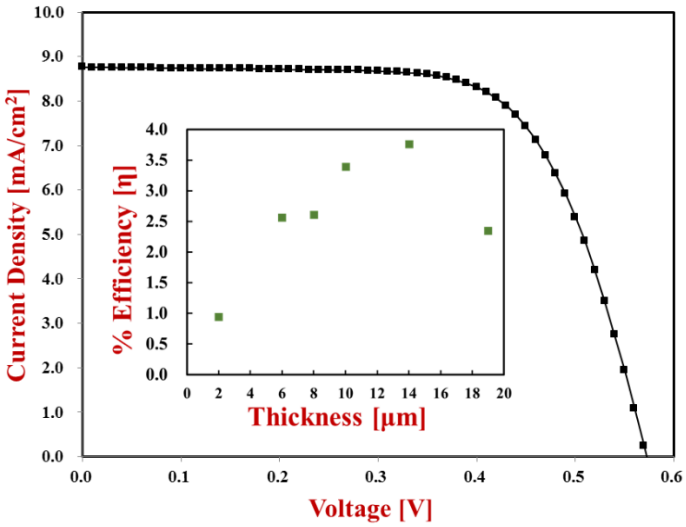

Figure 3. Photovoltaic characteristic of DSSC with TiO_2 layer thickness of 10 μm under simulated solar irradiation. Inset shows the thickness dependence of photoconversion efficiency

Table 2. Photovoltaic parameters for DSSC based on SQ-41 with varying thickness of the mesoporous TiO_2 layer.

Thickness	2 μm	6 μm	8 μm	10 μm	14 μm	19 μm
Efficiency (%)	0.94	2.57	2.61	3.39	3.76	2.35
FF	0.72	0.61	0.62	0.68	0.67	0.62
V_{oc} (V)	0.55	0.57	0.56	0.57	0.59	0.58
J_{sc} (mA/cm^2)	2.40	7.35	7.51	8.76	9.58	6.52

3.4. Influence of Nature of Electrolyte

Redox electrolyte plays a vital role in the dye regeneration during DSSC operation and affects all of photovoltaic parameters like J_{sc}, V_{oc} and FF finally controlling the η. Amongst several discovered electrolytes for DSSCs till date, iodine based redox couple I^-/I_3^- are still preferred for research laboratory and exhibited its dominance until 2010 [19]. This electrolyte works well with approximately all kinds of sensitizing dyes used in DSSCs. It is unlike to cobalt complex based redox shuttles needing specific dye design especially dyes bearing larger number of long alkyl chains [20]. It mainly contains the sources of I^- and I_3^- to form redox couple, I^- supplying ionic liquid for long term stability, some additives to tune the energetics of mesoporous TiO_2 and finally a suitable solvent. In this investigation, three different recipes of iodine based redox electrolyte (Electrolyte **A**, **B** and **C**) which have been most extensively utilized in DSSC research for Ru dyes have been attempted and their influence on photovoltaic performance was explored. In order to predict the main role played by electrolytes and its constituents, other DSSC fabrication parameters like thickness of mesoporous TiO_2 layer (12-13 μm), dye (SQ-41), CDCA to dye ratio (50), $TiCl_4$ surface treatments etc. were fixed

varying only the type of electrolyte. Figure 4 depicts the I-V characteristics of DSSCs using different types of electrolyte bearing I^-/I_3^- redox couple along with photovoltaic parameters shown in the table 3. A perusal of Fig. 4 and table 3 clearly corroborates that even under similar other DSSC fabrication parameters, only change in the recipe and components of iodine based redox electrolyte affects the overall photovoltaic performance. Only change in the concentration of TBP as additive and nature of ionic liquid for electrolyte **A** leads to enhancement of both of the observed J_{sc} and V_{oc} as compared to electrolyte **B** suggesting the importance of judicious selection of particular electrolyte system in order to achieve the optimum photo conversion efficiency.

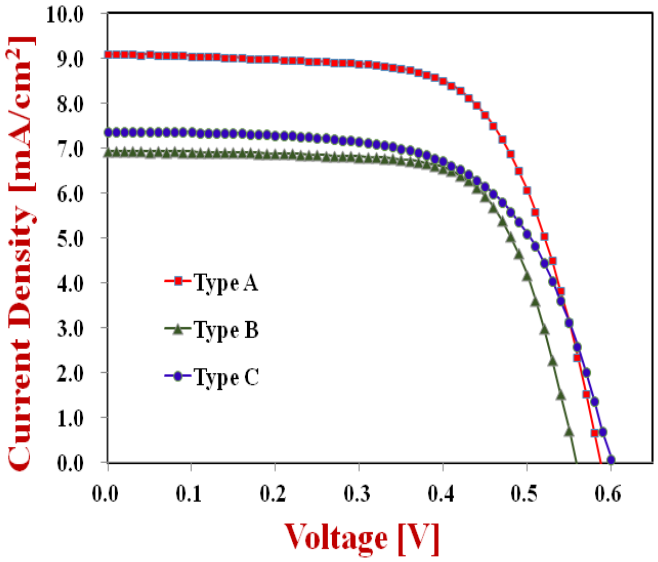

Figure 4. Photovoltaic characteristics of DSSC using SQ-41 in the presence of different iodine based redox electrolyte.

Table 2. Photovoltaic parameters for DSSC based on SQ-41 with different types of I^-/I_3^- based redox electrolytes

Electrolytes	Type-A	Type-B	Type-C
Efficiency (%)	3.50	2.70	2.77
FF	0.65	0.70	0.63
V_{oc} (V)	0.59	0.56	0.60
J_{sc} (mA/cm^2)	9.10	6.94	7.37

4. Conclusions

It has been demonstrated that control and optimization of DSSC fabrication parameters are highly desired in order to achieve optimum photoconversion efficiency for a particular class of dye sensitizer. Utilization of CDCA as coadsorber leads to enhanced photoconversion efficiency and 50-100 times of CDCA with respect to dye concentration was found to be optimum. $TiCl_4$ surface treatment was found to control the overall photoconversion efficiency and as compared to FTO layer, $TiCl_4$ treatment of mesoporous TiO_2 layer was found to play dominant role to achieve the best efficiency. Finally mesoporous TiO_2 layer having thickness in the range of 10-14 μm and iodine based redox electrolyte **A** was found to be optimum for DSSCs using far-red sensitive SQ-41 dye as photosensitizer.

Acknowledgments
One of the authors (SSP) would like express sincere thanks to Japan Society for the Promotion of Science (JSPS) for the financial support by Grant-in-Aid for Scientific Research (C) (Grant Number 26410206).

References

[1] Grätzel M 2009, *Acc. Chem. Res.* **42** 1788
[2] Kakiage K, Aoyama Y, Yano T, Otsuka T, Kyomen T, Unno M and Hanaya M 2014 *Chem. Commun. 50 6379*
[3] Wang M, Grätzel C, Zakeeruddin S M, Grätzel M 2012 *Energy Environ. Sci.* **5** 9394
[4] Mathew S, Yella A, Gao P, Humphry-Baker R, Curchod BF, Ashari-Astani N, Tavernelli I, Rothlisberger U, Nazeeruddin M K, Gratzel M 2014 *Nat. Chem.* **6** 242
[5] Gao F, Wang Y, Shi D, Zhang J, Wang M, Jing X, Humphry-Baker R, Wang P, Zakeeruddin S M, Grätzel M 2008 *J. Am. Chem. Soc*. **130** 10720
[6] Sreejith S, Carol P, Chithra P, Ajayaghosh A 2008 *J. Mater. Chem.* **18** 264
[7] Ito S, Murakami T N, Comte P, Liska P, Grätzel C, Nazeeruddin M K, Grätzel M 2008 *Thin Solid Films* **516** 4613
[8] Pandey S S, Inoue T, Fujikawa N, Yamaguchi Y, Hayase S 2010 *Thin Solid Films.* **519** 1066
[9] Morimoto T, Fujikawa N, Ogomi Y, Pandey S S, Ma T, Hayase S 2016 *J. Nanosci. Nanotechnol.* (In press)
[10] Hara K, Tachibana Y, Ohga Y, Shinpo A, Suga S, Sayama K, Sugihara H, Arakawa H 2013 *Sol. Energy Mater. Sol. Cells* **77** 89
[11] Yoshida Y, Tokashiki S, Kubota K, Shiratuchi R, Yamaguchi Y, Kono M, Hayase S 2008 *Sol. Energy Mater. Sol. Cells* **92** 646
[12] Gao F, Wang Y, Shi D, Zhang J, Wang M, Jing X, Humphry-Baker R, Wang P, Zakeeruddin S M, Grätzel M 2008 *J. Am. Chem. Soc*. **130** 10720
[13] Barbe C J, Arendse F, Comte P, Jirousek M, Lenzamann F, Shklover V, Grätzel M 1997 *J. Am. Ceram. Soc.* **80** 3157
[14] Sommeling P M, O'Regan B C, Haswell R R, Smit H J P, Bakker N. J, Smits J J T, Kroon J M, van Roosmalen J A M 2006 *J. Phys. Chem*. B **110** 19191
[15] Park N G, Schlichthorl G, Lagemaat J V D, Cheong H M, Mascarenhas A, Frank A J 1999 *J. Phys. Chem. B* **103** 3308
[16] Zeng L Y, Dai S Y, Wang K J, Pan X, Shi C W, Guo L 2004 *Chin. Phys. Lett.* **21** 835
[17] Man Gu Kang, Kwang Sun Ryu, Soon Ho Chang, Nam Gyu Park, Jin Sup Hong, Kang-Jin Kim 2004 *Bull. Korean Chem. Soc*. **25** 742
[18] Yamaguchi T, Uchida Y, Agatsuma S, Arakawa H 2009 *Sol. Energy Mater. Sol. Cells* **93** 733
[19] Jihuai W, Zhang L, Jianming L, Miaoliang H, Yunfang H, Leqing F and Genggeng L 2015 *Chem. Rev.* **115** 2136
[20] Zong X, liang M, Fan C, Tang K, Li G, Sun Z, Xue S 2012 *J. Phys. Chem. C*. **116** 11241